Noncoherent Multiuser Detection for Nonlinear Modulation Over the Rayleigh-Fading Channel

Artur Russ and Mahesh K. Varanasi, *Senior Member, IEEE*

***Abstract*—The jointly optimum noncoherent multiuser detector is obtained for nonlinear nonorthogonal modulation over the frequency nonselective Rayleigh-fading multiple-access channel. Upper and lower bounds on average bit-error probability are derived. While these bounds are numerically computable, they are too complicated to give insight into the relative influence of system parameters on the essential behavior of the bit-error rate. Hence this paper develops an asymptotic analysis of the average bit-error probability. In particular, it is shown that the upper and lower bounds are asymptotically convergent. An exact formula for the asymptotic efficiency of the optimum noncoherent detector is derived. Interestingly, the asymptotic efficiency is found to be positive and independent of the signal strengths of the interfering users. In contrast, the noncoherent detector which would be optimal in a single-user channel (the "conventional detector"), when used over the multiuser channel, has an asymptotic efficiency that is identically equal to zero no matter what the powers of the interferers may be. While the performance analysis of the optimum detector provides the fundamental limit on achievable error rate, the implementational complexity of the optimum detector is exponential in the number of users. As a low-complexity alternative, a decorrelative energy detector is also proposed and analyzed in terms of error probability and asymptotic efficiency.**

***Index Terms*—Code division multiaccess, error analysis, multiuser channels, multiuser detection, noncoherent detection, nonlinear modulation, Rayleigh fading.**

I. INTRODUCTION

CONSIDER a binary nonlinear signaling scheme where each of the K users transmits one of two nonorthogonal equi-energy signals to send one bit of information. After passing through a frequency-nonselective Rayleigh-fading channel (cf. [1]), the superposition of the K signals are assumed to arrive in symbol synchronism at the receiver. The complex baseband representation of the received signal is

$$r(t) = \sum_{m} \sum_{k=1}^{K} A_k(m) s_{kj_k(m)}(t - mT) + z(t) \qquad (1)$$

where $z(t)$ is the additive white Gaussian noise process with a power spectral density (one-sided) of σ^2, $j_k(m) \in \{1, 2\}$ denotes the mth information bit of user k, $s_{kj_k(m)}(t)$ is one of two (depending on the value of $j_k(m)$) complex-valued, unit-energy, possibly nonorthogonal signature signals of user k. We assume that these signals are such that, after matched filtering at the receiver, there is no intersymbol interference (ISI), i.e.,

$$\int s^*_{ki}(t - mT) s_{lj}(t - nT)\, dt = 0$$

whenever $m \neq n$. Signals which are time-limited to one symbol interval (i.e., $s_{kj}(t) = 0$ outside the interval $[0, T]$) are simple examples of such zero-ISI signals. More generally, the signals can be chosen to be linear combinations of pulses that satisfy the so-called generalized Nyquist criterion (cf. [2]). As a practical matter, the particular pulses chosen (that satisfy this criterion) must be of duration no greater than that over which the multiplicative fading remains constant. The $A_k(m)$'s are the channel fading parameters, assumed constant over the appropriate *signal* durations, and are modeled as being mutually independent (across users), zero-mean, complex Gaussian random processes. Let $E[|A_k|^2] = E_k$, so that E_k is user k's average energy per bit. Note that the assumption that the fading processes are constant over a signal duration is usually referred to as "slow" fading (cf. [3]).

While we focus attention on binary modulation in this paper, the results herein can be extended to the case of M-ary modulation. Note also that frequency-shift keying (FSK) and differential phase-shift keyed (DPSK) modulation are special cases of the model in (1). DPSK can be modeled with

$$s_{k1}(t) = p_k(t) + p_k(t - T/2)$$

and

$$s_{k2}(t) = p_k(t) - p_k(t - T/2)$$

where $p_k(t)$ is the kth users' transmitter pulse, assumed to satisfy the generalized Nyquist criterion with baud rate $2/T$. For example, $p_k(t)$ can be restricted to be time-limited to the interval $[0, T/2]$. In this case, the slow fading assumption implicit in (1) is that the fading process is essentially constant over two successive (differentially encoded) signal durations.

Our system model can also be seen as representing a coded system where the signals of a particular user are the waveforms that are used to represent individual codewords. While the binary modulation model restricts codes to having just 2-codewords, the analytical tools developed to study the asymptotic multiuser pairwise error probabilities in this paper can be used to analyze more general coded systems.

Manuscript received January 4, 1999; revised June 17, 2000. This work was supported by the U.S. National Science Foundation under Grants NCR-9406069 and ANI-9725778. The material in this paper was presented in part at the IEEE Personal, Indoor, Mobile Radio Communications Conference, Helsinki, Finland, September 1997 and at the IEEE Global Telecommun. Conference, Phoenix, AZ, November 1997.

A. Russ was with the University of Colorado, Boulder, CO 80309 USA. He is now with Infineon Technologies, Munich, Germany (e-mail: artur.russ@infineon.com).

M. K. Varanasi is with the Department of Electrical and Computer Engineering, University of Colorado, Boulder, CO 80309–0425 (e-mail: varanasi@schof.colorado.edu).

Communicated by U. Madhow, Associate Editor for Detection and Estimation.

Publisher Item Identifier S 0018-9448(01)00581-8.

In considering the optimum, decorrelative, and conventional detectors of this paper, it is not assumed that the channel fading parameters or their estimates are available at the receiver. Our results are, therefore, applicable to channels with any dependence in time of the fading processes, and particularly to applications in which the fading parameters are not explicitly estimated over multiple signal durations, either because they cannot be reliably estimated as in rapidly fading channels, or the extra complexity and cost of their estimation cannot be justified. The milder assumption is made that a simple statistical characterization of the fading parameters is available through a knowledge of the energies E_k.

Noncoherent multiuser detection for nonlinear nonorthogonal multipulse modulation was studied for the Gaussian multiple-access channel in [4]–[8], and for the Rayleigh-fading multiple-access channel in the abbreviated conference versions of this paper [9], [10]. Noncoherent detection for orthogonal modulation was considered in [11], [12]. Tutorial articles on coherent and differentially coherent multiuser detection for linear modulation are available (cf. [13], [14]). In particular, the multiuser Rician fading channel was studied in [15] and the Rayleigh-fading channel with perfect channel state information was examined in [16] and [17]. A recent textbook on multiuser detection [18] gives a brief account of nonlinear modulation based on the results of [4], [5], [7], [9], [10], and [12].

The rest of this paper is organized as follows. In Section II, we specify the optimum noncoherent detector and state the results for upper and lower bounds on average error probability. In Section III, which contains the key results of this paper, we analyze the bit-error probability of the optimum detector for high signal-to-noise ratios (SNRs). This leads to an exact formula for its asymptotic efficiency. In Section IV, we specify the conventional detector and obtain its error rate for finite and high SNRs. Since the complexity of the optimum detector may be too high, and the performance of the conventional detector very poor, a suboptimum decorrelative energy detector is proposed and analyzed in Section V. In Section VI, we present numerical examples that validate our analytical results. Section VII concludes this paper.

II. Optimum Noncoherent Detection

In this section, we obtain the jointly optimum noncoherent detector and the upper and lower bounds on error probability. Because of the assumption of zero ISI, we can restrict our attention to the transmission of a single bit from each user (with $m = 0$ in (1)). For convenience, we drop the time index as well.

The received signal $r(t)$ is first passed through a bank of $2K$ matched filters, matched to each of the signature signals $s_{kj_k}(t)$. Assuming that these signals are nonzero over the time interval $\mathcal{T}$, the output of the filter bank is a $2K$-dimensional complex vector $\boldsymbol{y}$ of sufficient statistics

$$\boldsymbol{y} = \int_{\mathcal{T}} r(t)\boldsymbol{s}^*(t)\,dt \tag{2}$$

with

$$\boldsymbol{s}(t) = (s_{11}(t), s_{12}(t), s_{21}(t), \ldots, s_{K2}(t))^T.$$

We define the signal correlation matrix

$$\boldsymbol{R} = \int_{\mathcal{T}} \boldsymbol{s}^*(t)\boldsymbol{s}^T(t)\,dt \in \boldsymbol{C}^{2K\times 2K}. \tag{3}$$

In this section, we let the waveforms in $\boldsymbol{s}(t)$ be linearly dependent so that $\boldsymbol{R}$ is positive semidefinite. We define the K-dimensional vector $\boldsymbol{b}$, with $b_k \in \{1, -1\}$, where $b_k = 1$ $(b_k = -1)$ means that the kth user employs its first (second) signal. Specific realizations of $\boldsymbol{b}$ (there are 2^K of them) are denoted through the index i of H_i, the ith hypothesis. We also use the notation $\boldsymbol{b}(H_i)$ to express the realization of $\boldsymbol{b}$ corresponding to H_i. This dual representation ($\boldsymbol{b}$ and H_i) is convenient to characterize the problem at hand.

With the above definitions, one can express the covariance matrix of the zero-mean Gaussian random vector $\boldsymbol{y}$ as

$$\boldsymbol{K}_{\boldsymbol{y}|H_i} = \boldsymbol{R}\hat{\boldsymbol{D}}^{H_i}\boldsymbol{R} + \sigma^2\boldsymbol{R}$$

where $\hat{\boldsymbol{D}}^{H_i}$ is a $2K \times 2K$ diagonal matrix, with diagonal elements given as

$$\begin{aligned}\hat{D}^{H_i}_{2k-12k-1} &= \frac{1}{2}\,E_k(1 + b_k(H_i))\\ \hat{D}^{H_i}_{2k2k} &= \frac{1}{2}\,E_k(1 - b_k(H_i)), \qquad k \in \{1, 2, \ldots, K\}.\end{aligned} \tag{4}$$

When we have K users, each employing two signals, the optimum decision rule, with optimality defined as the minimum probability of erronous joint decisions, will be a 2^K hypotheses testing problem. Assuming equiprobable input signals for each user, the maximum *a posteriori* rule is the maximum-likelihood rule [19]. Consequently, for a given vector $\boldsymbol{y}$, the optimum multiuser maximum-likelihood detector ϕ^{rmopt} selects the hypothesis $H_{\hat{i}}$ according to

$$\phi^{\text{opt}}\colon \hat{i} = \arg \min_{1\le i\le 2^K} \left\{\boldsymbol{y}^\dagger \boldsymbol{K}^{-1}_{\boldsymbol{y}|H_i}\boldsymbol{y} + \ln\left(\det\left(\boldsymbol{K}_{\boldsymbol{y}|H_i}\right)\right)\right\} \tag{5}$$

where $\dagger$ denotes the complex-conjugate transpose operation. The extension of (5) to M-ary modulation is straightforward. Note that the generic problem of testing hypotheses where the observations are zero-mean Gaussian random vectors with distinct covariance matrices arises in the context of detection of stochastic signals in single-user channels as well (cf. [19, Ch. 3]).

Without loss of generality, the performance analysis in this paper is done for the first user. An upper bound on the conditional error probability given H_i results from invoking a union bound, and a lower bound from considering for every H_i, just that H_j which differs only in b_1, or equivalently the K-dimensional error vector $\boldsymbol{e}^{ij} = (\pm 1 \quad 0 \quad 0\cdots 0)^T$, with $\boldsymbol{e}^{ij}$ defined element-wise as $e^{ij}_k = 1/2(b_k(H_i) - b_k(H_j))$. Error vectors which have only one nonzero entry at position one will be of special importance in the asymptotic analysis. We refer to them as unity-weight error vectors.

Let us consider the evaluation of the conditional pair-wise error probability that H_j gets chosen over H_i when H_i is true (henceforth denoted as $P_{H_i \to H_j}$). It follows from (5) that we must evaluate the probability of the event that the Hermitian form

$$f_{ij} \triangleq \boldsymbol{y}^\dagger(\boldsymbol{K}_{\boldsymbol{y}|H_j}^{-1} - \boldsymbol{K}_{\boldsymbol{y}|H_i}^{-1})\boldsymbol{y}$$

is less than or equal to the real-valued threshold $\hat{c}_{ij}$ defined as

$$\hat{c}_{ij} \triangleq \ln\left(\det(\boldsymbol{K}_{\boldsymbol{y}|H_i})/\det(\boldsymbol{K}_{\boldsymbol{y}|H_j})\right). \tag{6}$$

Therefore, we obtain the characteristic function [Laplace transform of the probability density function (pdf)] of the Hermitian form

$$f_{ij} = \boldsymbol{y}^\dagger(\boldsymbol{K}_{\boldsymbol{y}|H_j}^{-1} - \boldsymbol{K}_{\boldsymbol{y}|H_i}^{-1})\boldsymbol{y}$$

as being (cf. [1])

$$G_{f_{ij}}(s) = \frac{\prod_{k=1}^{N}\left(\frac{1}{\hat{\lambda}_{ij}^k}\right)^{n_k}}{\prod_{k=1}^{N}\left(\frac{1}{\hat{\lambda}_{ij}^k}+s\right)^{n_k}} \tag{7}$$

where $\hat{\lambda}_{ij}^k$ is the kth eigenvalue from the set of N nonzero eigenvalues with multiplicity n_k of the matrix

$$\hat{\boldsymbol{C}}_{H_iH_j} = \boldsymbol{K}_{\boldsymbol{y}|H_i}\boldsymbol{K}_{\boldsymbol{y}|H_j}^{-1} - \boldsymbol{I}. \tag{8}$$

After an inverse Laplace transform to obtain the pdf, and integrating over appropriate ranges, we obtain

$$\begin{aligned} P_{H_i\to H_j} = &\sum_{\substack{k \\ \hat{\lambda}_{ij}^k>0}} \frac{1}{\prod_{\substack{l=1\\l\neq k}}^{2K}\left(1-\frac{\hat{\lambda}_{ij}^l}{\hat{\lambda}_{ij}^k}\right)}\left(1-\exp\left(-\frac{\hat{c}_{ij}}{\hat{\lambda}_{ij}^k}\right)\right) \\ &+ \sum_{\substack{k \\ \hat{\lambda}_{ij}^k<0}} \frac{1}{\prod_{\substack{l=1\\l\neq k}}^{2K}\left(1-\frac{\hat{\lambda}_{ij}^l}{\hat{\lambda}_{ij}^k}\right)} \end{aligned} \tag{9}$$

for $\hat{c}_{ij} \geq 0$, and assuming distinct eigenvalues. For $\hat{c}_{ij} < 0$ the corresponding probability becomes

$$P_{H_i\to H_j} = \sum_{\substack{k \\ \hat{\lambda}_{ij}^k<0}} \frac{1}{\prod_{\substack{l=1\\l\neq k}}^{2K}\left(1-\frac{\hat{\lambda}_{ij}^l}{\hat{\lambda}_{ij}^k}\right)} \exp\left(-\frac{\hat{c}_{ij}}{\hat{\lambda}_{ij}^k}\right). \tag{10}$$

With this result for each individual conditional error probability, the above-mentioned upper and lower bounds on the overall bit-error probability become

$$P \leq \frac{1}{2^K}\sum_{i=1}^{2^K}\sum_{\substack{j=1\\ \text{s.t. } b_1(H_i)\neq b_1(H_j)}}^{2^K} P_{H_i\to H_j} \triangleq P_U \tag{11}$$

$$P \geq \frac{1}{2^K}\sum_{\substack{i=1\\ \boldsymbol{e}^{ij}=(\pm 100\cdots 0)^T}}^{2^K} P_{H_i\to H_j} \triangleq P_L. \tag{12}$$

III. Asymptotic Behavior of Error Probability

In this section and the rest of the paper, we will assume that the signals in $\boldsymbol{s}(t)$ are linearly independent so that the correlation matrix $\boldsymbol{R}$ is invertible. In attempting to gain insight into the asymptotic behavior of the error probability, it turns out that the terms become more revealing if we reformulate the optimum multiuser decision rule (5) in the following way:

$$\phi^{\text{opt}}: \hat{i} = \arg\min_{1\leq i\leq 2^K}\left\{\boldsymbol{z}^\dagger\boldsymbol{K}_{\boldsymbol{z}|H_i}^{-1}\boldsymbol{z} + \ln\left(\det\left(\boldsymbol{K}_{\boldsymbol{z}|H_i}\right)\right)\right\} \tag{13}$$

where the equivalence with (5) results from introducing

$$\boldsymbol{z} = \boldsymbol{R}^{-1}\boldsymbol{y} \tag{14}$$

$$\boldsymbol{K}_{\boldsymbol{z}|H_i} = \boldsymbol{R}^{-1}\boldsymbol{K}_{\boldsymbol{y}|H_i}\boldsymbol{R}^{-1} = \sigma^2(\gamma\boldsymbol{D}^{H_i} + \boldsymbol{Q}) \tag{15}$$

with $\boldsymbol{Q} \triangleq \boldsymbol{R}^{-1}$, and recognizing that $\ln(\det(\boldsymbol{R}))$ is independent of H_i. In (15), we factored out σ^2, to explicitly introduce $\gamma = E_1/\sigma^2$, the SNR of user one. The matrix $\boldsymbol{D}^{H_i}$ in (15) differs from $\hat{\boldsymbol{D}}^{H_i}$ by the multiplicative factor $1/E_1$.

Let us define

$$c_{ij} \triangleq \ln(\det(\boldsymbol{K}_{\boldsymbol{z}|H_i})/\det(\boldsymbol{K}_{\boldsymbol{z}|H_j}))$$

and let λ_{ij}^k denote the eigenvalues of the matrix (the superscript k is an index, not an exponent)

$$\boldsymbol{C}_{H_iH_j} \triangleq \boldsymbol{K}_{\boldsymbol{z}|H_i}\boldsymbol{K}_{\boldsymbol{z}|H_j}^{-1} - \boldsymbol{I}. \tag{16}$$

In the following subsections, we first obtain the high γ characterization of the thresholds c_{ij} and the eigenvalues λ_{ij}^k. Following that, we show that the error probability is asymptotically dominated by the unity-weight error vectors, which finally allows us to show that P_U and P_L are asymptotically coincident. This also allows us to compute the asymptotic efficiency.

A. Asymptotics of c_{ij}

We first establish an asymptotic expression for c_{ij} which can also be written as

$$c_{ij} = \ln\left(\det\left(\tilde{\boldsymbol{K}}_{\boldsymbol{z}|H_i}\right)\Big/\det\left(\tilde{\boldsymbol{K}}_{\boldsymbol{z}|H_j}\right)\right). \tag{17}$$

where $\tilde{\boldsymbol{K}}_{\boldsymbol{z}|H_i} \triangleq \sigma^{-2}\boldsymbol{K}_{\boldsymbol{z}|H_i}$. For any hypothesis H_i, the determinant $\det(\tilde{\boldsymbol{K}}_{\boldsymbol{z}|H_i})$ is a polynomial of degree K in γ. In the computation of c_{ij}, the ratio of two such determinants is involved. Hence, the limit of c_{ij} as $\gamma\to\infty$ is obtained as

$$\bar{c}_{ij} \triangleq \lim_{\gamma\to\infty} c_{ij} = \ln\left(\frac{a_K\left(\det\left(\tilde{\boldsymbol{K}}_{\boldsymbol{z}|H_i}\right)\right)}{a_K\left(\det\left(\tilde{\boldsymbol{K}}_{\boldsymbol{z}|H_j}\right)\right)}\right) \tag{18}$$

where $a_K(\det(\tilde{\boldsymbol{K}}_{\boldsymbol{z}|H_i}))$ denotes the coefficient associated with γ^K of the polynomial $\det(\tilde{\boldsymbol{K}}_{\boldsymbol{z}|H_i})$.

A closed-form expression for $\bar{c}_{ij}$ defined in (18) can be obtained as follows: if we assume $\boldsymbol{b}(H_i)$ to have all entries equal to unity and define the energy ratios $r_k \triangleq E_k/E_1$, the asymptotic approximation of the matrix $\tilde{\boldsymbol{K}}_{\boldsymbol{z}|H_i}$ has the form

$$\tilde{\boldsymbol{K}}_{\boldsymbol{z}|H_i} \approx \begin{pmatrix} \gamma & Q_{12} & Q_{13} & Q_{14} & Q_{15} & \cdots & Q_{12K} \\ Q_{12}^* & Q_{22} & Q_{23} & Q_{24} & Q_{25} & \cdots & Q_{22K} \\ Q_{13}^* & Q_{23}^* & r_2\gamma & Q_{34} & Q_{35} & \cdots & Q_{32K} \\ Q_{14}^* & \cdot & \cdot & Q_{44} & \cdot & \cdots & Q_{42K} \\ Q_{15}^* & \cdot & \cdot & \cdot & r_3\gamma & \cdots & Q_{52K} \\ \vdots & \vdots & \vdots & \vdots & \vdots & \ddots & \vdots \\ Q_{12K}^* & \cdot & \cdot & \cdot & \cdot & \cdots & Q_{2K2K} \end{pmatrix}. \tag{19}$$

In general (for any hypothesis), one can identify the permutation matrix that will rearrange the elements of the asymptotic approximation of $\tilde{\boldsymbol{K}}_{\boldsymbol{z}|H_i}$ given in (19) into

$$\begin{pmatrix} \boldsymbol{K}_{ul}^{H_i} & \boldsymbol{K}_{ur}^{H_i} \\ \boldsymbol{K}_{ll}^{H_i} & \boldsymbol{K}_{lr}^{H_i} \end{pmatrix} \tag{20}$$

where the diagonal elements of $\boldsymbol{K}_{ul}^{H_i}$ are linearly proportional to γ (note that each of the submatrices in (20) is of dimension $K \times K$). Consequently

$$a_K\left(\det\left(\tilde{\boldsymbol{K}}_{\boldsymbol{z}|H_i}\right)\right) = \det\left(\boldsymbol{K}_{lr}^{H_i}\right) a_K\left(\det\left(\boldsymbol{K}_{ul}^{H_i} - \boldsymbol{K}_{ur}^{H_i}\left(\boldsymbol{K}_{lr}^{H_i}\right)^{-1}\boldsymbol{K}_{ll}^{H_i}\right)\right) \tag{21}$$

$$= \det\left(\boldsymbol{K}_{lr}^{H_i}\right)\prod_{i=2}^{K} r_i \tag{22}$$

so that

$$\bar{c}_{ij} = \ln\left(\frac{\det\left(\boldsymbol{K}_{lr}^{H_i}\right)}{\det\left(\boldsymbol{K}_{lr}^{H_j}\right)}\right). \tag{23}$$

B. Asymptotics of Eigenvalues

In this subsection, we are concerned with the asymptotics of the eigenvalues of $\boldsymbol{C}_{H_iH_j}$ defined in (16). We will first establish properties for the eigenvalues which are true for any SNR. This will determine only part of the eigenvalues. To characterize the rest, we have to use an asymptotic argument for high SNR.

For any two hypotheses H_i and H_j, the covariance matrices $\boldsymbol{K}_{\boldsymbol{z}|H_i}$ and $\boldsymbol{K}_{\boldsymbol{z}|H_j}$ can be rearranged in a way that the elements corresponding to users indexed by all such k for which $b_k(H_i) \neq b_k(H_j)$ are in the upper left corner, so that

$$\boldsymbol{K}_{\boldsymbol{z}|H_i} = \begin{pmatrix} \boldsymbol{K}_{11}^{H_i} & \boldsymbol{K}_{12} \\ \boldsymbol{K}_{12}^{\dagger} & \boldsymbol{K}_{22} \end{pmatrix} \tag{24}$$

$$\boldsymbol{K}_{\boldsymbol{z}|H_j} = \begin{pmatrix} \boldsymbol{K}_{11}^{H_j} & \boldsymbol{K}_{12} \\ \boldsymbol{K}_{12}^{\dagger} & \boldsymbol{K}_{22} \end{pmatrix}. \tag{25}$$

For an error vector with weight e, the matrix $\boldsymbol{K}_{11}^{H_i}$ will be $2e \times 2e$. Using the fact that the second block row of the matrix $\boldsymbol{K}_{\boldsymbol{z}|H_i}\boldsymbol{K}_{\boldsymbol{z}|H_j}^{-1}$ is equal to the second block row of the matrix $\boldsymbol{K}_{\boldsymbol{z}|H_j}\boldsymbol{K}_{\boldsymbol{z}|H_j}^{-1}$ (which in turn is the identity matrix), it follows that the matrix $\boldsymbol{C}_{H_iH_j}$ with the same partitioning as in (24) and (25), takes on the form

$$\boldsymbol{C}_{H_iH_j} = \begin{pmatrix} \left(\boldsymbol{C}_{H_iH_j}\right)_{11} & \left(\boldsymbol{C}_{H_iH_j}\right)_{12} \\ \boldsymbol{0} & \boldsymbol{0} \end{pmatrix} \tag{26}$$

where the $\boldsymbol{0}$'s are all-zero matrices of appropriate dimensions. Thus, for an error vector of weight e, $2(K-e)$ eigenvalues are equal to 0 and the nonzero eigenvalues coincide with those of $(\boldsymbol{C}_{H_iH_j})_{11}$. When investigating the asymptotic behavior of $(\boldsymbol{C}_{H_iH_j})_{11}$, the crucial step is to determine the inverse $\boldsymbol{K}_{\boldsymbol{z}|H_i}^{-1}$ for high SNR.

The inverse of any $N \times N$ invertible matrix $\boldsymbol{M}$ can be computed as

$$\boldsymbol{M}^{-1} = (\det(\boldsymbol{M}))^{-1}\boldsymbol{A}^T \tag{27}$$

with elements $A_{kl} = (-1)^{k+l}\det(\boldsymbol{M}_{kl})$, where $\boldsymbol{M}_{kl}$ is a matrix that results by striking out the kth row and lth column of $\boldsymbol{M}$. A_{kl} is called the *cofactor* of the matrix element M_{kl}. The matrix $\boldsymbol{A}^T$ with entries A_{kl} as defined is called the *adjugate* of $\boldsymbol{M}$ [20]. Whenever it is not clear from which matrix a cofactor is computed, we add it as an argument, as in $A_{kl}(\boldsymbol{M})$.

We introduce the following notation: $\{L, p\}$ means that the polynomial p is of degree L. By applying the formula for the inverse of a matrix in (27) to the matrix given in (19), and using the notation just described, we have (28) as shown at the bottom of this page with

$$A_{kl} = (-1)^{k+l}\det((\boldsymbol{K}_{\boldsymbol{z}|H_i}^{\mathrm{eq}})_{kl})$$

$$\boldsymbol{K}_{\boldsymbol{z}|H_i}^{-1} \sim \frac{1}{\{K, D_i\}} \begin{pmatrix} \{K-1, A_{11}\} & \{K-1, A_{12}\} & \left\{K-2, \frac{1}{r_2}A_{13}\right\} & \{K-1, A_{14}\} & \cdots & \{K-1, A_{12K}\} \\ \{K-1, A_{21}\} & \{K, A_{22}\} & \left\{K-1, \frac{1}{r_2}A_{23}\right\} & \{K, A_{24}\} & \cdots & \{K, A_{22K}\} \\ \left\{K-2, \frac{1}{r_2}A_{31}\right\} & \left\{K-1, \frac{1}{r_2}A_{32}\right\} & \left\{K-1, \frac{1}{r_2}A_{33}\right\} & \left\{K-1, \frac{1}{r_2}A_{34}\right\} & \cdots & \left\{K-1, \frac{1}{r_2}A_{32K}\right\} \\ \{K-1, A_{41}\} & \{K, A_{42}\} & \left\{K-1, \frac{1}{r_2}A_{43}\right\} & \{K, A_{44}\} & \cdots & \{K, A_{42K}\} \\ \vdots & \vdots & \vdots & \vdots & \ddots & \vdots \\ \{K-1, A_{2K1}\} & \{K, A_{2K2}\} & \left\{K-1, \frac{1}{r_2}A_{2K3}\right\} & \{K, A_{2K4}\} & \cdots & \{K, A_{2K2K}\} \end{pmatrix}^T \tag{28}$$

and

$$D_i = \det(\boldsymbol{K}^{\mathrm{eq}}_{\boldsymbol{z}|H_i})$$

$\boldsymbol{K}^{\mathrm{eq}}_{\boldsymbol{z}|H_i}$ is defined as the covariance matrix of $\boldsymbol{z}|H_i$ for equal energies among all users. So, for each $\boldsymbol{K}_{\boldsymbol{z}|H_i}$ we have associated an equal energy version $\boldsymbol{K}^{\mathrm{eq}}_{\boldsymbol{z}|H_i}$. This notation is useful, because it enables us to explicitly recognize the dependence of the asymptotic form of the inverse of the matrix $\boldsymbol{K}_{\boldsymbol{z}|H_i}$ on the energy ratios r_k.

In general, the highest degree in γ of an entry $A_{kl}(\boldsymbol{K}_{\boldsymbol{z}|H_i})$ is

- K, if $(\boldsymbol{K}^{eq}_{\boldsymbol{z}|H_i})_{kk} \neq \gamma$ and $(\boldsymbol{K}^{eq}_{\boldsymbol{z}|H_i})_{ll} \neq \gamma$;
- $K-1$, if $(\boldsymbol{K}^{eq}_{\boldsymbol{z}|H_i})_{kk} \neq \gamma$ xor $(\boldsymbol{K}^{eq}_{\boldsymbol{z}|H_i})_{ll} \neq \gamma$;
- $K-2$, if $(\boldsymbol{K}^{eq}_{\boldsymbol{z}|H_i})_{kk} = \gamma$ and $(\boldsymbol{K}^{eq}_{\boldsymbol{z}|H_i})_{ll} = \gamma$;

where we used "xor" to denote a logic exclusive-or.

In the next step we use this insight into $\boldsymbol{K}^{-1}_{\boldsymbol{z}|H_i}$ to investigate the asymptotic behavior of the matrix $(\boldsymbol{C}_{H_iH_j})_{11}$, in whose eigenvalues we are interested. It can be shown that for the general case of an error weight e with $e \in \{1, 2, \ldots, K\}$, the asymptotic approximation of the matrix $(\boldsymbol{C}_{H_iH_j})_{11}$ is given by (29), shown at the bottom of this page, where an entry 0 implies that the term in its place has highest exponent of γ no greater than -1. We also assumed without loss of generality that all e nonzero elements of $\boldsymbol{e}$ are equal to -1. The constants c_{mn}, with $m, n \in \{1, 2, \ldots e\}$ are constants that are all independent of γ.

We are interested in the characteristic polynomial

$$c(\lambda) \triangleq \det(\lambda \boldsymbol{I} - (\boldsymbol{C}_{H_iH_j})_{11}).$$

We use Laplace's expansion and retain only terms which will give coefficients that involve γ^e since only such terms matter in the asymptotic analysis. Thus, we obtain the characteristic polynomial as shown in (30) and (31) at the bottom of this page, where the matrix $\boldsymbol{P}$ is implicitly defined in the last equation. From (30) it is easily seen that -1 is an eigenvalue with multiplicity e. The other e eigenvalues are positive, which follows from viewing the $e \times e$ matrix $\boldsymbol{P}$, as the product of the diagonal matrix $\boldsymbol{D} = \mathrm{diag}(1\, r_2 \cdots r_e)$ and a principal submatrix $\boldsymbol{S}$ of the positive-definite matrix $(\boldsymbol{K}^{eq}_{\boldsymbol{z}|H_j})^{-1}$ which is thus also positive-definite. The positivity of the eigenvalues of $\boldsymbol{P}$ follow from Sylvester's law of inertia [20]. As every element of $\boldsymbol{P}$ is proportional to γ all eigenvalues are hence also proportional to γ. Moreover, these eigenvalues depend on the energy ratios $r_2 \cdots r_e$.

In general then, we conclude that for any arbitrary error vector of weight e (by appropriately renumbering the users and their signals, and following the above argument for the particular case of the error vector with all nonzero elements equal to -1), the eigenvalues of $\boldsymbol{C}_{H_iH_j}$ always have the following structure for high SNR: there are e eigenvalues equal to -1, e eigenvalues positive and proportional to γ, and $2(K-e)$ eigenvalues equal to 0. Moreover, the positive eignevalues are a function of the energy ratios of the interfering users whose indices are the same as those of the nonzero elements of the error vector.

Consider the important example of a unity-weight error vector $\boldsymbol{e}^{ij} = (-1 \quad 0 \quad \cdots \quad 0)^T$. For the asymptotic form of $(\boldsymbol{C}_{H_iH_j})_{11}$ we obtain

$$\left(\boldsymbol{C}_{H_iH_j}\right)_{11} \approx \begin{pmatrix} -1 & c_1 \\ c_2 & \alpha_{ij}\gamma \end{pmatrix} \tag{32}$$

with

$$\alpha_{ij} = a_K\left(A_{22}\left(\boldsymbol{K}^{\mathrm{eq}}_{\boldsymbol{z}|H_j}\right)\right) \Big/ a_K\left(\det\left(\boldsymbol{K}^{\mathrm{eq}}_{\boldsymbol{z}|H_j}\right)\right).$$

Note that α_{ij} is positive, since both the numerator and the denominator are positive, which in turn is a consequence of $\boldsymbol{K}^{\mathrm{eq}}_{\boldsymbol{z}|H_j}$ being positive-definite. The asymptotic eigenvalues of $(\boldsymbol{C}_{H_iH_j})_{11}$ are, therefore, easily established to be -1 and $\alpha_{ij}\gamma$. Note the important property that the asymptotic eigenvalues

$$\left(\boldsymbol{C}_{H_iH_j}\right)_{11} \approx \begin{pmatrix} -1 & c_{11} & 0 & c_{12} & 0 & \cdots & c_{1e} \\ c_{21} & \frac{a_K(A_{22})}{a_K(D_j)}\gamma & c_{22} & \frac{a_K(A_{42})}{a_K(D_j)}\gamma & c_{23} & \cdots & \frac{a_K(A_{(2e)2})}{a_K(D_j)}\gamma \\ 0 & c_{31} & -1 & c_{32} & 0 & \cdots & c_{3e} \\ \vdots & \vdots & \vdots & \vdots & \vdots & \ddots & \vdots \\ c_{(2e)1} & r_e\frac{a_K(A_{2(2e)})}{a_K(D_j)}\gamma & c_{(2e)2} & r_e\frac{a_K(A_{4(2e)})}{a_K(D_j)}\gamma & c_{(2e)3} & \cdots & r_e\frac{a_K(A_{(2e)(2e)})}{a_K(D_j)}\gamma \end{pmatrix} \tag{29}$$

$$c(\lambda) \approx (\lambda+1)^e \det \begin{pmatrix} \lambda - \frac{a_K(A_{22})}{a_K(D_j)}\gamma & -\frac{a_K(A_{42})}{a_K(D_j)}\gamma & \cdots & -\frac{a_K(A_{(2e)2})}{a_K(D_j)}\gamma \\ -r_2\frac{a_K(A_{24})}{a_K(D_j)}\gamma & \lambda - r_2\frac{a_K(A_{44})}{a_K(D_j)}\gamma & \cdots & -r_2\frac{a_K(A_{(2e)4})}{a_K(D_j)}\gamma \\ \vdots & \vdots & \ddots & \vdots \\ -r_e\frac{a_K(A_{2(2e)})}{a_K(D_j)}\gamma & -r_e\frac{a_K(A_{4(2e)})}{a_K(D_j)}\gamma & \cdots & \lambda - r_e\frac{a_K(A_{(2e)(2e)})}{a_K(D_j)}\gamma \end{pmatrix} \tag{30}$$

$$\triangleq (\lambda+1)^e \det(\lambda\boldsymbol{I} - \boldsymbol{P}) \tag{31}$$

for unit-weight error vectors in this case are independent of the signal strengths of the interfering users.

C. Dominance of Unity-Weight Error Vectors

We will show in this section that we only have to consider unity-weight error vectors (which lead to eigenvalues with multiplicity one) when considering the high SNR case. For $e = 1$ and $\boldsymbol{e}^{ij} = (-1 \quad 0 \quad \cdots 0)^T$ and for $\overline{c}_{ij} \ge 0$, it is easily shown that

$$P_{(H_i \to H_j)_1} \approx \frac{1}{\alpha_{ij}\gamma} + 1 - \exp\left(-\frac{(\overline{c}_{ij})_1}{\alpha_{ij}\gamma}\right) \tag{33}$$

where the subscript 1 with $P_{(H_i \to H_j)}$ and $\overline{c}_{ij}$ stands for unity weight. In the rest of this subsection, we will deal with only the case $\overline{c}_{ij} \ge 0$. The conclusions for the case $\overline{c}_{ij} < 0$ are the same.

For higher than unity-weight sequences, we have to deal with multiple eigenvalues. Equation (7) represents the characteristic function for the Hermitian form f_{ij}, with possibly multiple nonzero eigenvalues. In our situation, we have the eigenvalue -1 of multiplicity e and e distinct eigenvalues which are positive and proportional to γ.

For an arbitrary weight e error vector, with $e > 1$, it can be shown that, asymptotically, the terms corresponding to the eigenvalue -1 decrease as γ^{-e} and the terms corresponding to the e eigenvalues $\alpha_{ij}^k\gamma$, $k \in \{1, 2, \ldots, e\}$ (note, the superscript k is an index, not an exponent) can be written as the sum

$$\sum_{k=1}^{e} \frac{(\alpha_{ij}^k)^{e-1}}{\prod_{\substack{l=1 \\ l \ne k}}^{e} (\alpha_{ij}^k - \alpha_{ij}^l)} \left(1 - \exp\left(-\frac{(\overline{c}_{ij})_e}{\alpha_{ij}^k\gamma}\right)\right). \tag{34}$$

The proof of the above statements can be found in Appendix A.

To prove that the unity-weight error vectors dominate the error probability for high SNR we have to show that

$$\lim_{\gamma \to \infty} \frac{P_{(H_i \to H_j)_e}}{P_{(H_i \to H_j)_1}} = 0 \tag{35}$$

for all $e > 1$. With (33), (34), and the fact that the terms corresponding to the e-times repeated eigenvalue -1 decrease like γ^{-e}, we obtain for (35), after applying l'Hospital's rule

$$\lim_{\gamma \to \infty} \frac{P_{(H_i \to H_j)_e}}{P_{(H_i \to H_j)_1}} = \frac{(\overline{c}_{ij})_e \sum_{k=1}^{e} \frac{(\alpha_{ij}^k)^{e-2}}{\prod_{\substack{l=1 \\ l \ne k}}^{e} (\alpha_{ij}^k - \alpha_{ij}^l)}}{\frac{1}{\alpha_{ij}}((\overline{c}_{ij})_1 + 1)}. \tag{36}$$

So, (35) is true if the numerator in (36) is zero. This is a direct consequence of the lemma proved in Appendix B.

Equation (35) is a fundamental result, as it says, that for high SNR, the error probability for a specific user is dominated by the unity-weight error vectors. The same result is also true for coherent detection in a Rayleigh-fading channel with known [16], [17] or imperfectly (but optimally) estimated fading parameters [21]. However, the proof of the dominance of the unity-weight error vector in the noncoherent case of this paper requires a more delicate analysis.

We have thus established that the upper and lower bounds on the error probability introduced in Section II converge asymptotically.

D. Asymptotic Efficiency

In the multiuser channel, one is also interested in the performance degradation due to the interfering users rather than the background noise. A performance measure which captures this idea is the *asymptotic efficiency* (cf. [17], [22]), which for user k, is defined as

$$\eta_k = \sup\left\{0 \le \delta \le 1, \lim_{\sigma \to 0} \frac{P_k^M(E_k, \sigma)}{P^S(\delta E_k, \sigma)} \le 1\right\} \tag{37}$$

where $P_k^M(E_k, \sigma)$ is the error probability of user k in the multiuser setting and $P^S(\delta E_k, \sigma)$ is the minimum achievable error probability in a single-user channel where only user k is active with energy δE_k. The appropriate single-user scheme uses two nonorthogonal equi-energy signals and noncoherent detection. It can be established that, for high SNR, the single-user error probability becomes

$$P^S \approx \frac{1}{(1 - |R_{12}|^2)\gamma} \tag{38}$$

where R_{12} is the correlation between the two normalized signature signals.

For the optimum detector in the multiuser channel, we proved that for high SNR, it does not matter which bound we take to compute the asymptotic error probability. As the lower bound is easier to compute, we will use this to obtain an exact formula for asymptotic efficiency.

Consider conditional error probabilities for unity-weight error vectors. Using the asymptotic expressions for the eigenvalues derived in Section III-B we obtain

$$\begin{aligned} P_{ij} &\triangleq \frac{1}{2}(P_{H_i \to H_j} + P_{H_j \to H_i}) \\ &\approx \begin{cases} \frac{1}{2}\left(\frac{\overline{c}_{ij} + 1}{\alpha_{ij}\gamma} + \frac{e^{-\overline{c}_{ij}}}{\alpha_{ji}\gamma}\right), & \text{if } \overline{c}_{ij} \ge 0 \\ \frac{1}{2}\left(\frac{e^{\overline{c}_{ij}}}{\alpha_{ij}\gamma} + \frac{1 - \overline{c}_{ij}}{\alpha_{ji}\gamma}\right), & \text{if } \overline{c}_{ij} < 0 \end{cases} \end{aligned} \tag{39}$$

where $\alpha_{ij}\gamma$ ($\alpha_{ji}\gamma$) is the positive eigenvalue corresponding to the error event $H_i \to H_j$ ($H_j \to H_i$). We also used the property $\overline{c}_{ji} = -\overline{c}_{ij}$. We omit the subscript 1 with $P_{H_i \to H_j}$ and c_{ij}, because in this section, we deal only with unity-weight error vectors. Consider the following definition:

$$\eta_{ij} \triangleq \sup\left\{0 \le \delta \le 1, \lim_{\sigma \to 0} \frac{\frac{1}{2}(P_{H_i \to H_j} + P_{H_j \to H_i})}{P^S(\delta E_k, \sigma)} \le 1\right\}. \tag{40}$$

Using (39), (38) we obtain

$$\eta_{ij} = \begin{cases} \dfrac{2}{\left(\frac{\overline{c}_{ij}}{\alpha_{ij}} + \frac{1}{\alpha_{ij}} + \frac{1}{\alpha_{ji}}\exp(-\overline{c}_{ij})\right)(1 - |R_{12}|^2)}, & \text{if } \overline{c}_{ij} \ge 0 \\ \dfrac{2}{\left(\frac{-\overline{c}_{ij}}{\alpha_{ji}} + \frac{1}{\alpha_{ji}} + \frac{1}{\alpha_{ij}}\exp(\overline{c}_{ij})\right)(1 - |R_{12}|^2)}, & \text{if } \overline{c}_{ij} < 0. \end{cases} \tag{41}$$

The asymptotic efficiency of the optimum detector for the first user (denoted as η_1^{opt}) using the definition in (37) can be shown to be the harmonic mean of the 2^{K-1} terms of the type given in (41), i.e.,

$$\eta_1^{\mathrm{opt}} = 2^{K-1}\left(\sum_{i;\, b_1(H_i)=1} (\eta_{ij})^{-1}\right)^{-1}. \tag{42}$$

Note that j stands for hypothesis H_j that is different from H_i only in the first user's symbol.

It remains to specify an explicit formula for α_{ij}. When the two hypotheses differ in only the first user's symbol, it can be shown that

$$\alpha_{ij} = \frac{1}{Q_{kk} - \boldsymbol{x}_j^T \left(\overline{\boldsymbol{K}}_{lr}^{H_j}\right)^{-1} \boldsymbol{x}_j^\star} \tag{43}$$

where

$$k = \begin{cases} 1, & \text{if } b_1(H_j) = -1 \\ 2, & \text{if } b_1(H_j) = 1 \end{cases} \tag{44}$$

and where $\overline{\boldsymbol{K}}_{lr}^{H_j}$ and $\boldsymbol{x}_j$ are defined through the partition

$$\boldsymbol{K}_{lr}^{H_j} = \begin{pmatrix} Q_{kk} & \boldsymbol{x}_j^T \\ \boldsymbol{x}_j^\star & \overline{\boldsymbol{K}}_{lr}^{H_j} \end{pmatrix}. \tag{45}$$

Combining (41), (42), (23), and (43) together yields the sought result

$$\begin{aligned}\eta_1^{\text{opt}} = \frac{2^{K-1}}{1-|R_{12}|^2} \Bigg(\sum_{i;\, b_1(H_i)=1} & \left(1 + \frac{|\overline{c}_{ij}|}{2}\right) \\ & \cdot \min \left\{ Q_{22} - \boldsymbol{x}_i^T \left(\overline{\boldsymbol{K}}_{lr}^{H_i}\right)^{-1} \boldsymbol{x}_i^\star, \right. \\ & \left. Q_{11} - \boldsymbol{x}_j^T \left(\overline{\boldsymbol{K}}_{lr}^{H_j}\right)^{-1} \boldsymbol{x}_j^\star \right\} \Bigg)^{-1}\end{aligned} \tag{46}$$

where

$$\overline{c}_{ij} = \ln \left(\frac{Q_{22} - \boldsymbol{x}_i^T \left(\overline{\boldsymbol{K}}_{lr}^{H_i}\right)^{-1} \boldsymbol{x}_i^\star}{Q_{11} - \boldsymbol{x}_j^T \left(\overline{\boldsymbol{K}}_{lr}^{H_j}\right)^{-1} \boldsymbol{x}_j^\star} \right). \tag{47}$$

For the single-user channel, the above formula is equal to unity as it should be. For the two-user channel, the asymptotic efficiency can be simplified as

$$\begin{aligned}\eta_1^{\text{opt, 2u}} = & \frac{2}{1-|R_{12}|^2} \\ & \cdot \Bigg[\left(1 + \frac{|c_1|}{2}\right) \min \left\{ Q_{11} - Q_{44}^{-1}|Q_{14}|^2, \right. \\ & \qquad \left. Q_{22} - Q_{44}^{-1}|Q_{24}|^2 \right\} \\ & + \left(1 + \frac{|c_2|}{2}\right) \min \left\{ Q_{11} - Q_{33}^{-1}|Q_{13}|^2, \right. \\ & \qquad \left. Q_{22} - Q_{33}^{-1}|Q_{23}|^2 \right\} \Bigg]^{-1}\end{aligned} \tag{48}$$

where

$$c_1 = \ln \left(\frac{Q_{22}Q_{44} - |Q_{24}|^2}{Q_{11}Q_{44} - |Q_{14}|^2} \right)$$

and

$$c_2 = \ln \left(\frac{Q_{22}Q_{33} - |Q_{23}|^2}{Q_{11}Q_{33} - |Q_{13}|^2} \right). \tag{49}$$

E. Near–Far Resistance

Let us define the near–far resistance (cf. [18]) as the worst case asymptotic efficiency over the relative interfering signal strengths, i.e.,

$$\overline{\eta}_1 = \inf_{r_2, r_3, \ldots, r_K} \eta_1. \tag{50}$$

From (43), we see that the asymptotic eigenvalues $\alpha_{ij}\gamma$ are independent of the energies of the interfering users for unity-weight error vectors. From (23), this independence is also seen to be true for $\overline{c}_{ij}$. Hence we have the remarkable result that the asymptotic efficiency in (46) is also equal to the near–far resistance. Furthermore, from (41) it is easily seen that each term in (42) is positive and, therefore, that the asymptotic efficiency (and hence near–far resistance) is positive. Thus, the optimum detector is near–far resistant. This means that the asymptotic performance of the optimum multiuser detector rivals the optimum detector in a single-user channel where the latter uses η_1^{opt} times the energy in the multiuser channel. The error-rate asymptote of the optimum detector decays inversely with SNR. Furthermore, η_1^{opt} is independent of the powers of the interfering users so that the error-rate asymptote is invariant to interfering signal strengths.

The independence of the asymptotic efficiency of the optimum detector to the interfering signal energies was also shown for coherent detection in the Rayleigh-fading channel [16], [17]. It should, however, be noted that there is a significant difference between the coherent and the noncoherent problems: whereas for the coherent case, the dominance of a unity-weight error vector means that the signals of the interfering users can essentially be assumed to be completely known at the receiver, so that the independence of the asymptotic efficiency makes intuitive sense (which is also why asymptotic efficiency is equal to unity in this case); that this independence even holds for the noncoherent case—in spite of the fact that the revelation of the information transmitted by all interfering users does *not* imply that the interfering signals are perfectly known because of the associated random and unknown complex amplitudes—is an all the more interesting fact.

IV. The Conventional Detector

A detector which applies the single-user decision rule in a multiuser channel is called the conventional detector. We will derive its error probability and investigate it for high SNR. It will be shown that the conventional detector suffers from a flooring of its error probability.

If it were falsely to assume that only the first user is active, then the sufficient statistics are the two outputs of the matched filters for that user, i.e., the first two elements of $\boldsymbol{y}$ which we denote as $\boldsymbol{y}_C$. The optimum single-user decision rule based on the same false assumption is, therefore,

$$\boldsymbol{y}_C^\dagger \left(\boldsymbol{K}_{\boldsymbol{y}_S|H_1}^{-1} - \boldsymbol{K}_{\boldsymbol{y}_S|H_0}^{-1} \right) \boldsymbol{y}_C \triangleq \Lambda^C \underset{H_1}{\overset{H_0}{\gtrless}} 0 \tag{51}$$

with $\boldsymbol{K}_{\boldsymbol{y}_S|H_0}$ and $\boldsymbol{K}_{\boldsymbol{y}_S|H_1}$ being the appropriate single-user covariance matrices in a fictitious single-user channel where only the first user is active.

A. Error Probability

The covariance matrix of $\boldsymbol{y}_C$ conditioned on $\boldsymbol{b}$, which we denote as $\boldsymbol{C}_{\boldsymbol{y}_C|\boldsymbol{b}}$, is given as

$$\boldsymbol{C}_{\boldsymbol{y}_C|\boldsymbol{b}} = \begin{pmatrix} \boldsymbol{r}_1^T \boldsymbol{D}_{|\boldsymbol{b}}^{H_i} \boldsymbol{r}_1^\star + \sigma^2 & \boldsymbol{r}_1^T \boldsymbol{D}_{|\boldsymbol{b}}^{H_i} \boldsymbol{r}_2^\star + R_{12}\sigma^2 \\ \left(\boldsymbol{r}_1^T \boldsymbol{D}_{|\boldsymbol{b}}^{H_i} \boldsymbol{r}_2^\star + R_{12}\sigma^2\right)^\star & \boldsymbol{r}_2^T \boldsymbol{D}_{|\boldsymbol{b}}^{H_i} \boldsymbol{r}_2^\star + \sigma^2 \end{pmatrix} \tag{52}$$

where we introduced the vector $\boldsymbol{r}_i^T$ as the ith row of $\boldsymbol{R}$, $i \in \{1, 2\}$, and moreover, $\boldsymbol{D}_{|\boldsymbol{b}}^{H_i}$ is defined as in (15) with the dependence of H_i on $\boldsymbol{b}$ made explicit.

By symmetry, the bit-error rate of the conventional detector is equal to the conditional error probability given that the first user transmits the first signal. Therefore, averaging over the bits of the interfering users, we have

$$\begin{aligned} P^C &= P^C_{H_0 \to H_1} = \frac{1}{2^{K-1}} \sum_{\substack{\boldsymbol{b} \\ b_1 = 1}} \Pr\left(\Lambda^C < 0 | \boldsymbol{b}\right) \\ &\triangleq \frac{1}{2^{K-1}} \sum_i P^C_{(H_0 \to H_1)_i}. \end{aligned} \tag{53}$$

Each term $P^C_{(H_0 \to H_1)_i}$ of this probability can be expressed in terms of the two eigenvalues of the matrix $\boldsymbol{C}_{\boldsymbol{y}_C|\boldsymbol{b}}(\boldsymbol{K}^{-1}_{\boldsymbol{y}_S|H_1} - \boldsymbol{K}^{-1}_{\boldsymbol{y}_S|H_0})$, whose properties we will investigate. It can be shown that

$$\begin{aligned} &\boldsymbol{C}_{\boldsymbol{y}_C|\boldsymbol{b}}(\boldsymbol{K}^{-1}_{\boldsymbol{y}_S|H_1} - \boldsymbol{K}^{-1}_{\boldsymbol{y}_S|H_0}) \\ &\quad = \frac{\gamma}{1+\gamma} \begin{pmatrix} \gamma \boldsymbol{r}_1^T \boldsymbol{D}_{|\boldsymbol{b}}^{H_i} \boldsymbol{r}_1^\star + 1 & \gamma \boldsymbol{r}_1^T \boldsymbol{D}_{|\boldsymbol{b}}^{H_i} \boldsymbol{r}_2^\star + R_{12} \\ \gamma \boldsymbol{r}_1^T \boldsymbol{D}_{|\boldsymbol{b}}^{H_i} \boldsymbol{r}_2^\star + R_{21} & \gamma \boldsymbol{r}_2^T \boldsymbol{D}_{|\boldsymbol{b}}^{H_i} \boldsymbol{r}_2^\star + 1 \end{pmatrix} \\ &\qquad \cdot \begin{pmatrix} 1 & 0 \\ 0 & -1 \end{pmatrix}. \end{aligned} \tag{54}$$

The second matrix on the right-hand side of the above equation has eigenvalues 1 and -1. We continue to have one negative and one positive eigenvalue if this matrix is premultiplied by the first matrix on the right-hand side since the latter is positive-definite. Thus, one of the eigenvalues of $\boldsymbol{C}_{\boldsymbol{y}_C|\boldsymbol{b}}(\boldsymbol{K}^{-1}_{\boldsymbol{y}_S|H_1} - \boldsymbol{K}^{-1}_{\boldsymbol{y}_S|H_0})$ is positive and one is negative. For high SNR, we have

$$\begin{aligned} &\boldsymbol{C}_{\boldsymbol{y}_C|\boldsymbol{b}}(\boldsymbol{K}^{-1}_{\boldsymbol{y}_S|H_1} - \boldsymbol{K}^{-1}_{\boldsymbol{y}_S|H_0}) \\ &\quad \approx \gamma \begin{pmatrix} \boldsymbol{r}_1^T \boldsymbol{D}_{|\boldsymbol{b}}^{H_i} \boldsymbol{r}_1^\star & \boldsymbol{r}_1^T \boldsymbol{D}_{|\boldsymbol{b}}^{H_i} \boldsymbol{r}_2^\star \\ \boldsymbol{r}_1^T \boldsymbol{D}_{|\boldsymbol{b}}^{H_i} \boldsymbol{r}_2^\star & \boldsymbol{r}_2^T \boldsymbol{D}_{|\boldsymbol{b}}^{H_i} \boldsymbol{r}_2^\star \end{pmatrix} \begin{pmatrix} 1 & 0 \\ 0 & -1 \end{pmatrix}. \end{aligned} \tag{55}$$

Note that both eigenvalues are linear in γ for high SNR. But this means that each term $P^C_{(H_0 \to H_1)_i}$ in (53) takes on the form

$$P^C_{(H_0 \to H_1)_i} \approx \frac{\alpha_{2_i}}{\alpha_{1_i} + \alpha_{2_i}} \tag{56}$$

for high SNR, where we used $\lambda_{1_i} \approx \alpha_{2_i}\gamma$ and $\lambda_{2_i} \approx -\alpha_{2_i}\gamma$, $\alpha_{l_i} > 0$. Hence, for high SNR, each term $P^C_{(H_0 \to H_1)_i}$ in (53) approaches a *constant*. This shows that the conditional error probability for the conventional detector $P^C_{H_0 \to H_1}$ becomes independent of SNR for high SNR and exhibits a flooring of the error rate. Hence, the asymptotic efficiency of the conventional detector is identically equal to zero. This phenomenon occurs no matter what the energies of the interfering users are, as long as at least one of them is strictly positive. This is a more negative result than for the conventional detector for linear modulation in a Gaussian channel where it is known that when the interfering user energies are sufficiently weak, the conventional detector does not exhibit an error floor and that it can indeed even outperform suboptimum multiuser detectors such as the decorrelator for such operating points. The conventional approach is thus even worse for nonlinear modulation over fading channels than it is for the Gaussian channel.

V. The Noncoherent Decorrelative Energy Detector

The implementation of the optimum noncoherent detector requires the computation of as many quadratic forms as the number of hypotheses. Hence the complexity of the optimum detector appears to be exponential in the number of users. On the other hand, the conventional detector requires the computation of only two quadratic forms per user but its performance is unacceptable. In this section, we seek a complexity-constrained detector that approaches the performance of the optimum detector at least for lightly correlated signals. In particular, we consider strategies that are not much more complex to implement than the conventional detector. To this end, we adopt the approach of decorrelative detection for nonlinear modulation as proposed by the authors in [4] and [7] in the context of the Gaussian multiuser channel.

In nonlinear modulation, the superposition of signals transmitted by the various users lies in a signal subspace that depends on the particular choice of information symbols transmitted. This subspace is one of 2^K K-dimensional subspaces depending on which of the 2^K realizations of the K information bits are transmitted. It is suggested in [4] and [7] that the signal space be viewed as an expanded $2K$-dimensional space that is spanned by the $2K$ signals of all users. This expanded signal space is invariant to the information bits transmitted so that a decorrelative front-end is easily specified. The key problems that emerge are those of postdecorrelative detector design and analysis. Three near–far resistant solutions to such problems were obtained for the Gaussian channel in [4] and [7].

The idea of noncoherent decorrelation described above can be applied to the Rayleigh-fading channel. This is achieved by formally writing the received signal as that of a pseudo-linear scheme

$$r(t) = \sum_{k=1}^{K} A_k(\alpha_k s_{k1}(t) + \beta_k s_{k2}(t)) + z(t), \qquad t \in [0, T] \tag{57}$$

with

$$(\alpha_k, \beta_k) \in F_k = \{(1, 0), (0, 1)\}.$$

Then, the vector of sufficient statistics $\boldsymbol{y}$ defined in (2) can be expressed as

$$\boldsymbol{y} = \boldsymbol{R}\boldsymbol{A}\kappa + \boldsymbol{n} \tag{58}$$

with

$$\begin{aligned} \kappa &= (\alpha_1, \beta_1, \alpha_2, \beta_2, \ldots, \alpha_K, \beta_K)^T \in \{(1, 0), (0, 1)\}^K \\ \boldsymbol{A} &= \mathrm{diag}(A_1, A_1, A_2, \ldots, A_K) \in \boldsymbol{C}^{2K \times 2K} \end{aligned}$$

and $\boldsymbol{n}$ being zero-mean Gaussian with covariance matrix $\sigma^2 \boldsymbol{R}$. Now, as in channels with linear modulation, the correlation matrix $\boldsymbol{R}$ is independent of which signal is employed by each user.

Therefore, the decorrelation operation becomes independent of the transmitted symbols and the actual realizations of the fading parameters.

The decision vector $\boldsymbol{z}_1$, consisting of the first two elements of $\boldsymbol{R}^{-1}\boldsymbol{y}$ (without loss of generality, the analysis is done for user one) is complex, zero-mean, and Gaussian with covariance matrix

$$\boldsymbol{K}_{\boldsymbol{z}_1|H_i} = \sigma^2 \left[\gamma \begin{pmatrix} \alpha_1 & 0 \\ 0 & \beta_1 \end{pmatrix} + \begin{pmatrix} Q_{11} & Q_{12} \\ Q_{12}^* & Q_{22} \end{pmatrix} \right] \tag{59}$$

with $\boldsymbol{Q} = \boldsymbol{R}^{-1}$ and $\gamma = E_1/\sigma^2$, the SNR of user one. We denote by H_0 (H_1) the hypothesis that user one transmits the first (second) signal. Focusing attention only on $\boldsymbol{z}_1$, the minimum error probability detector is easily shown to be

$$\boldsymbol{z}_1^\dagger \left(\boldsymbol{K}_{\boldsymbol{z}_1|H_1}^{-1} - \boldsymbol{K}_{\boldsymbol{z}_1|H_0}^{-1} \right) \boldsymbol{z}_1 \underset{H_1}{\overset{H_0}{\gtrless}} c_D \tag{60}$$

with

$$c_D = \ln \left(\det \left(\boldsymbol{K}_{\boldsymbol{z}_1|H_0} \right) / \det(\boldsymbol{K}_{\boldsymbol{z}_1|H_1} \right).$$

The detector described by (60) will be called the Noncoherent Decorrelative Energy Detector (NDED). It can as such be implemented for the detection of a particular user, with a pair of filters that tune out the interfering users' signals whatever information they transmit, followed by the computation of the quadratic form in (60). The complexity is, therefore, essentially that of a single-user optimum detector for nonorthogonal binary modulation.

A. Error Probability

The model for $\boldsymbol{z}_1$ in (59) also arises in a single-user Rayleigh-fading channel over which nonorthogonal binary modulation is employed and where the effective energies of the two signals are unequal. Thus, the error-rate analysis of the NDED in this section also serves to provide the fundamental limit on the error rate achievable in such a general single-user channel.

The bit-error probability of the NDED in (60) is given as

$$P^D = \frac{1}{2} \left(P_{H_0 \to H_1}^D + P_{H_1 \to H_0}^D \right) \tag{61}$$

where $P_{H_i \to H_j}^D$ denotes the conditional probability that H_i is mistaken for H_j.

Each conditional error rate is of the general form

$$\Pr(\boldsymbol{x}^\dagger \boldsymbol{F} \boldsymbol{x} < c), \tag{62}$$

where $\boldsymbol{F}$ is any 2×2 indefinite Hermitian matrix, c is a real constant, and $\boldsymbol{x}$ is a bivariate, zero-mean, complex, Gaussian random vector with positive definite covariance matrix $\boldsymbol{K}$. We have encountered such probabilities in the analysis of the optimum detector.

The conditional error rate $P_{H_0 \to H_1}^D$ can be completely specified in terms of the constant c_D and the eigenvalues of the matrix $\boldsymbol{C}_{H_0 H_1} = \boldsymbol{K}_{\boldsymbol{z}_1|H_0} \boldsymbol{K}_{\boldsymbol{z}|H_1}^{-1} - \boldsymbol{I}$. Similarly, $P_{H_1 \to H_0}^D$ depends on the constant c_D and the eigenvalues of the matrix $\boldsymbol{C}_{H_1 H_0} = \boldsymbol{K}_{\boldsymbol{z}_1|H_1} \boldsymbol{K}_{\boldsymbol{z}|H_0}^{-1} - \boldsymbol{I}$. It can be shown that the two eigenvalues of $\boldsymbol{C}_{H_0 H_1}$ are real-valued, one of which is positive and the other negative (and hence distinct). Let us denote these eigenvalues as α_+ and α_-. A similar result is also true for $\boldsymbol{C}_{H_1 H_0}$. Let its positive and negative eigenvalue be denoted as β_+ and β_-, respectively. It is possible to obtain analytical expressions for these eigenvalues but they are unwieldy. Using the form of pairwise error rates given in (9) and (10), it can be shown that (assuming $c_D \geq 0$)

$$\begin{aligned} P^D = \frac{1}{2} \Bigg[&\frac{\alpha_+}{\alpha_+ - \alpha_-} \left(1 - \exp\left(-\frac{c_D}{\alpha_+} \right) \right) \\ &+ \frac{\alpha_-}{\alpha_- - \alpha_+} + \frac{\beta_-}{\beta_- - \beta_+} \exp\left(\frac{c_D}{\beta_-} \right) \Bigg]. \end{aligned} \tag{63}$$

The error probability in the case when $c_D < 0$ can be similarly specified.

B. Asymptotic Error Probability

While (63) gives an exact expression for the error rate of the NDED, it remains unclear as to how that error rate behaves relative to, say, the minimum error probability in a single-user channel or the error rate of the optimum detector. In this subsection, we derive a simple asymptotic expression for the error probability of the NDED and subsequently obtain its asymptotic efficiency. The analysis technique is similar to the one used for the analysis of the optimum detector.

In the high-SNR regime, the matrices $\boldsymbol{C}_{H_0 H_1}$ and $\boldsymbol{C}_{H_1 H_0}$ in whose eigenvalues we are interested, are approximately

$$\boldsymbol{C}_{H_0 H_1} \approx \begin{pmatrix} \frac{\gamma}{Q_{11}} & -\frac{Q_{12}}{Q_{11}} \\ \frac{Q_{12}^*}{Q_{11}} & -1 \end{pmatrix} \tag{64}$$

$$\boldsymbol{C}_{H_1 H_0} \approx \begin{pmatrix} -1 & \frac{Q_{12}}{Q_{22}} \\ -\frac{Q_{12}^*}{\gamma Q_{22}} & \frac{\gamma}{Q_{22}} \end{pmatrix}. \tag{65}$$

From these matrices it is easily derived that for $\boldsymbol{C}_{H_0 H_1}$, the asymptotic expressions for the eigenvalues are $\alpha_- \approx -1$ and $\alpha_+ \approx \gamma/Q_{11}$. The asymptotic eigenvalues of $\boldsymbol{C}_{H_1 H_0}$ are $\beta_- \approx -1$ and $\beta_+ \approx \gamma/Q_{22}$. It should be noted that the second eigenvalue is positive for both hypotheses because $\boldsymbol{Q}$ is positive-definite. Finally, c_D admits the asymptotic expression

$$\bar{c}_D = \lim_{\gamma \to \infty} c_D = \ln(Q_{22}/Q_{11}).$$

Distinguishing the two cases $\bar{c}_D \geq 0$ and $\bar{c}_D < 0$ we get the following expressions for the error probability of user one:

$$P^D \approx \frac{Q_{11}}{\gamma} \left(1 + \frac{\bar{c}_D}{2} \right) \tag{66}$$

for $\bar{c}_D \geq 0$, and

$$P^D \approx \frac{Q_{22}}{\gamma} \left(1 - \frac{\bar{c}_D}{2} \right) \tag{67}$$

for $\bar{c}_D < 0$. Thus, the bit error rate of the NDED depends inversely on the SNR as does the bit-error rate of the optimum detector in a single-user channel. Moreover, our asymptotic analysis is such that it gives the correct constant of proportionality in the inverse SNR term.

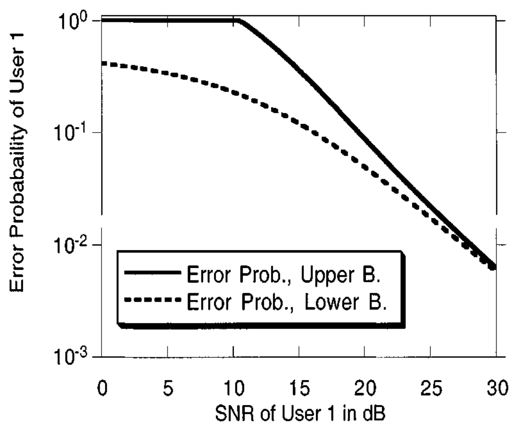

Fig. 1. The upper and lower bounds on error probability of the optimum detector—an illustration of asymptotic tightness of bounds.

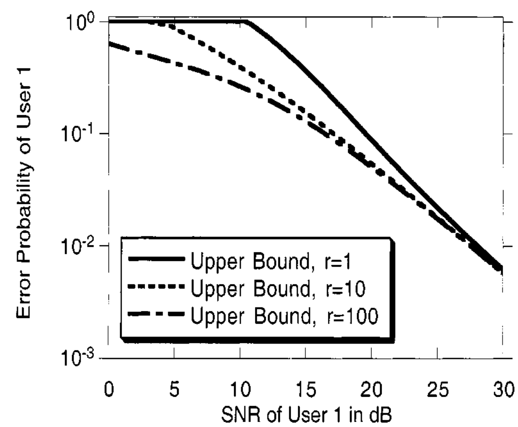

Fig. 2. Upper bounds on error probability of the optimum detector—invariance of high SNR performance to interferers' signal strengths ($r = E_i/E_1$, the interferer-to-desired-user-energy ratio).

Using the definition of asymptotic efficiency in (37) and the asymptotic error rates of the NDED in (66) and (67), one easily obtains the asymptotic efficiency of the NDED as

$$\eta^D = \begin{cases} \dfrac{2}{(\overline{c}_D Q_{11} + 2Q_{11})(1 - |R_{12}|^2)}, & \text{if } \overline{c}_D \geq 0 \\ \dfrac{2}{(2Q_{22} - \overline{c}_D Q_{22})(1 - |R_{12}|^2)}, & \text{if } \overline{c}_D < 0. \end{cases} \tag{68}$$

Note that although the expressions for single-user and decorrelator error probabilities in (38), (66), and (67) are only asymptotically correct and we thus used the $\approx$ symbol, the terms for asymptotic efficiency are exact results.

The asymptotic efficiency of the NDED is strictly positive and independent of the interfering signal strengths. Hence, its near–far resistance is equal to the asymptotic efficiency.

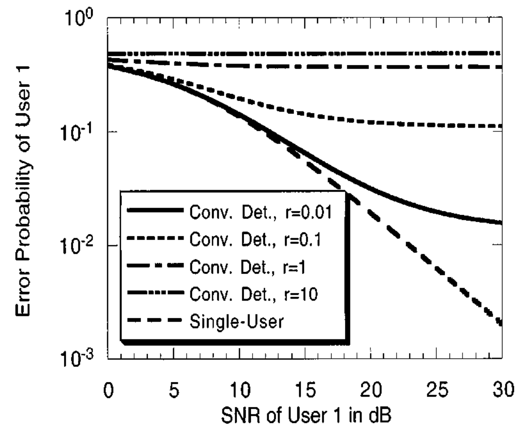

Fig. 3. Error probability of the conventional detector versus single-user channel performance—illustration of error-rate floors.

VI. Numerical Results

The central result of this paper was the convergence of the upper and lower bounds on the error probability of the optimum detector for high SNR. Fig. 1 demonstrates this behavior for a four-user case, with fairly highly correlated signals. To characterize the correlatedness of the signal set, we introduce the parameter β defined as the mean of the magnitudes of the off-diagonal elements of the signal correlation matrix. In this example $\beta = 0.76$. The signal correlation matrix itself is obtained by an algorithm given in [23].

We have shown the interesting result that the high-SNR error probability of the optimum detector for a particular user is effectively independent of the energies of the interfering users. This is illustrated in Fig. 2, where we plotted the upper bound on error probability for three different ratios r of interferers' energy to desired user's energy for a four-user channel. The signal correlation matrix was chosen to be the same as that of Fig. 1. Notice that as the interfering signal strengths increase, the error-rate bound decreases. This may seem contrary to what one might initially expect. However, such a result should not be surprising because with high interfering signal strengths, there is less uncertainty about those signals which, in turn, implies that such signals can be more effectively "subtracted" from the received signal.

In Fig. 3, we plot the error probability for the conventional detector. The single-user channel error rate (i.e., when $r_k = 0$ for $k = 2, \ldots, K$) is included for comparison. The performance of the conventional detector is depicted for various interfering user-to-desired-user-energy ratios r, with the SNR among the interfering users being equal. This figure is also consistent with our analytical results in that the error rate of the conventional detector exhibits an irreducible floor with increasing SNR.

Fig. 4 illustrates the error probabilities of the noncoherent decorrelative energy decorrelator (NDED). The correlation between the signals is assumed to be as in previous figures. For the sake of comparison, the bounds on the error rates of the joint optimum detector as well as the minimum achievable single-user error rate are also shown. It is seen in the figure that the gap between the optimum detector and the NDED may be acceptable in this example.

In Fig. 5, we plot the asymptotic efficiencies of the joint optimum detector and the NDED for the first user as a function of the parameter ρ for a two-user channel with correlation matrix $\boldsymbol{R}$ with $R_{kl} = \rho^{|k-l|}$ for all entries except R_{12} which we fix at 0.5 (so that the reference single-user channel remains unchanged as ρ is varied). Curiously, there is only a mild degradation of the NDED relative to the optimum detector over the range of values of valid ρ where $\boldsymbol{R}$ is positive definite.

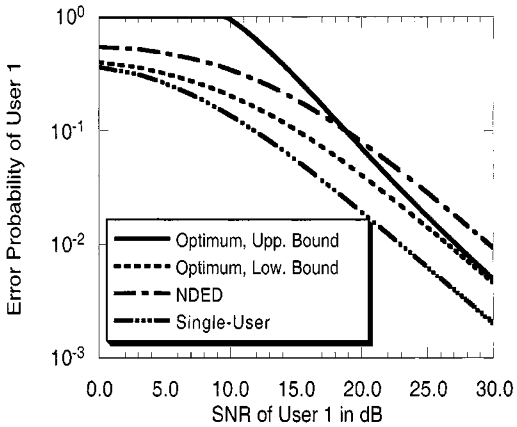

Fig. 4. Error rate comparison of the optimum and suboptimum (NDED) detectors relative to single-user performance.

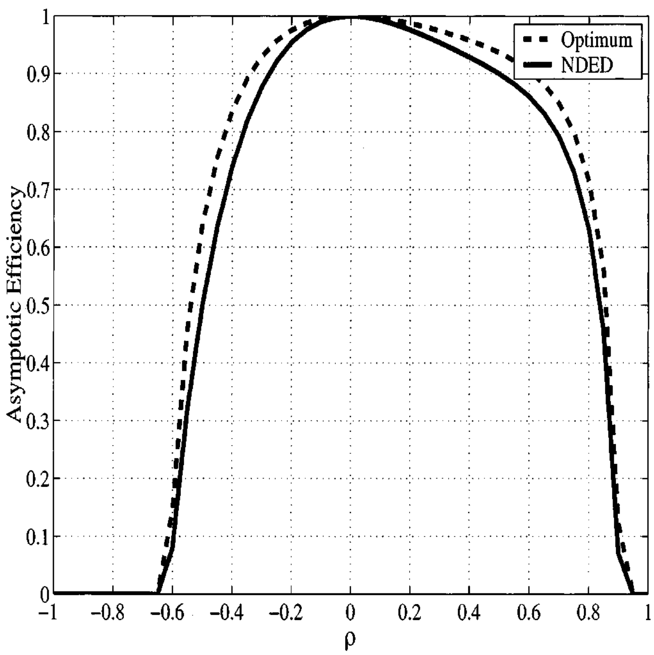

Fig. 5. Asymptotic efficiency comparison of the optimum detector and the NDED for a two-user channel with $R_{kl} = \rho^{|k-l|}$ for all entries except that $R_{12} = 0.5$.

Fig. 6 contains the same information as Fig. 5, but for a different two-user channel where the elements of $\boldsymbol{R}$ are given as $R_{12} = 0.5$ as before, but the rest of the $R_{kl} = \rho$ for $k \neq l$ ($R_{kk} = 1\,\forall k$). This figure illustrates the point that there can be a substantial difference in the error rates between the optimum detector and the NDED. It is seen in this example for $\rho = 0.8$, that the asymptotic efficiency of the optimum detector is twice that of the NDED (a 3-dB gap). The asymptotic efficiencies are positive over the range of values of ρ for which $\boldsymbol{R}$ is positive-definite.

VII. Conclusion

Optimum and suboptimum noncoherent multiuser detection for the nonselective Rayleigh-fading channel is studied. Upper and lower bounds on average error rate are obtained for the optimum detector. The main focus of this paper was

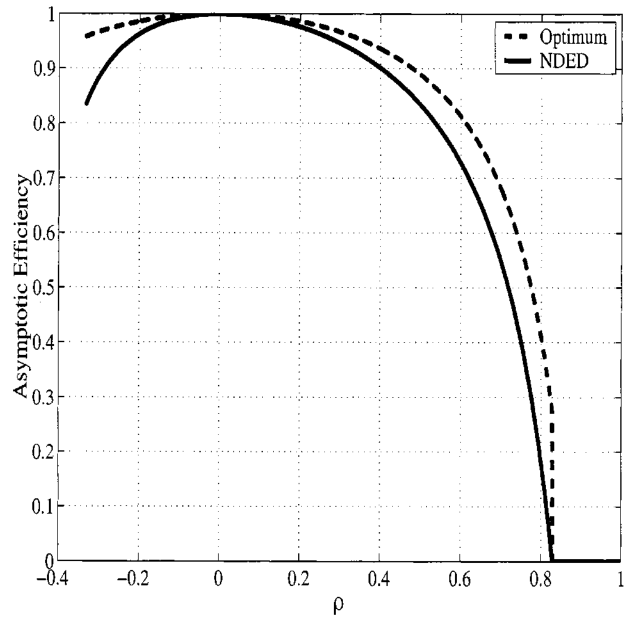

Fig. 6. Asymptotic efficiency comparison of the optimum detector and the NDED for a two-user channel with $R_{kl} = \rho$ for all $k \neq l$ except that $R_{12} = 0.5$.

on deriving formulas for the asymptotic (high-SNR) average bit-error probability of the optimum detector. It is also shown that this asymptotic error rate for each user decays as the inverse of that user's SNR and is independent of the interfering signal strengths. A closed-form expression for the asymptotic efficiency of the optimum detector is also derived. The conventional detector (which would be optimal in a single-user channel) on the other hand is shown to have an asymptotic average error rate that approaches a constant due to multiple-access interference. Its asymptotic efficiency is identically equal to zero for any distribution of interfering signal strengths. To provide a suboptimum low-complexity alternative to the exponentially complex optimum detector, the noncoherent decorrelative energy detector is proposed. A complete performance analysis of this detector is given in terms of the exact- and high-SNR bit-error probabilities as well as the asymptotic efficiency.

Appendix A

In this appendix, we show the validity of (34) and also demonstrate that for the general case of an error vector of weight e, the terms in the conditional error probability corresponding to the e-times repeated eigenvalue -1 are proportional to $1/\gamma^e$.

The characteristic function of f_{ij} with potentially multiple eigenvalues can be written using a partial fraction expansion as follows:

$$G^J_{f_{ij}}(s) = \frac{\prod_{k=1}^{N} \left(\frac{1}{\lambda^k_{ij}}\right)^{n_k}}{\prod_{k=1}^{N} \left(\frac{1}{\lambda^k_{ij}} + s\right)^{n_k}} = \sum_{k=1}^{N} \sum_{\nu=1}^{n_k} \frac{A_{k\nu}}{\left(s + \frac{1}{\lambda^k_{ij}}\right)^{\nu}}. \tag{69}$$

Each $A_{k\nu}$ can be determined as

$$A_{k\nu} = \frac{1}{(n_k-\nu)!}\frac{d^{n_k-\nu}}{ds^{n_k-\nu}}\left[\frac{\prod_{l=1}^{N}\left(\frac{1}{\lambda_{ij}^l}\right)^{n_l}}{\prod_{\substack{l=1\\ l\neq k}}^{N}\left(\frac{1}{\lambda_{ij}^l}+s\right)^{n_l}}\right]_{s=-1/\lambda_{ij}^k}. \tag{70}$$

Now, assuming that $c_{ij} \geq 0$, the conditional error probability $P_{H_i\to H_j}$ can be written as

$$P_{H_i\to H_j} = \sum_{\substack{k\\ \lambda_{ij}^k>0}}\sum_{\nu=1}^{n_k} A_{k\nu} \cdot\left[(\lambda_{ij}^k)^\nu - \sum_{m=0}^{\nu-1}\frac{1}{(\nu-1-m)!} \cdot(\lambda_{ij}^k)^{m+1}c_{ij}^{\nu-(m+1)}\exp\left(-\frac{c_{ij}}{\lambda_{ij}^k}\right)\right] \tag{71}$$

$$+ \sum_{\substack{k\\ \lambda_{ij}^k<0}}\sum_{\nu=1}^{n_k} A_{k\nu}(\lambda_{ij}^k)^\nu. \tag{72}$$

where we use the convention that $0! = 1$. The case $c_{ij} < 0$ can also be specified in a similar way but we omit the details here. In the special case under investigation, where the eigenvalue -1 has multiplicity e, the $A_{k\nu}$'s, with $\nu \in \{1, 2, \ldots, e\}$ can be written as

$$A_{k\nu} = \frac{1}{(e-\nu)!}\frac{d^{e-\nu}}{ds^{e-\nu}}\left[\frac{(-1)^e\prod_{l=1}^{e}\left(\frac{1}{\alpha_{ij}^l\gamma}\right)}{\prod_{l=1}^{e}\left(\frac{1}{\alpha_{ij}^l\gamma}+s\right)}\right]_{s=1}$$

$$= \frac{(-1)^e}{(e-\nu)!}\frac{d^{e-\nu}}{ds^{e-\nu}}\left[\frac{1}{\prod_{l=1}^{e}(1+\alpha_{ij}^l\gamma s)}\right]_{s=1}. \tag{73}$$

From the last equation it can be seen that the $A_{k\nu}$'s for all $\nu \in \{1, 2, \ldots, e\}$ are proportional to $1/\gamma^e$. Using this result and (71) it follows that the terms in the conditional error probability corresponding to the e-times repeated eigenvalues is proportional to $1/\gamma^e$.

Equation (34) results from substituting the e $A_{k\nu}$'s corresponding to the eigenvalues $\alpha_{ij}^l\gamma$ with $l \in \{1, 2, \ldots, e\}$. Those terms sum up to (34).

The case of $c_{ij} < 0$ can be handled similarly.

As an example, consider an error vector of weight 2. It is left as an exercise to the reader to verify that

$$P_{(H_i\to H_j)_2}^J \approx \frac{\alpha_{ij}^1}{\alpha_{ij}^1-\alpha_{ij}^2}\left(1-\exp\left(-\frac{(c_{ij})_2}{\alpha_{ij}^1\gamma}\right)\right) + \frac{\alpha_{ij}^2}{\alpha_{ij}^2-\alpha_{ij}^1}\left(1-\exp\left(-\frac{(c_{ij})_2}{\alpha_{ij}^2\gamma}\right)\right) + \frac{2}{\alpha_{ij}^1\alpha_{ij}^2\gamma^2}+\frac{1}{\alpha_{ij}^1\alpha_{ij}^2\gamma^2} \tag{74}$$

where the subscript 2 with $P_{(H_i\to H_j)}^J$ and c_{ij} stands for error weight 2. The last two terms with the γ^{-2} dependence result from the repeated eigenvalue -1.

APPENDIX B

Lemma: Given a set of L positive and distinct numbers $\{x_i\}_{i=1}^L$, it is true that

$$\sum_{i=1}^{L}\frac{x_i^{L-2}}{\prod_{\substack{j=1\\ j\neq i}}^{L}(x_i-x_j)} \triangleq \sum_{i=1}^{L} B_i \equiv 0. \tag{75}$$

Proof: Let us define the function $g(x)$

$$g(x) \triangleq \frac{x^{L-2}}{\prod_{i=1}^{L}(x-x_i)} \tag{76}$$

and perform a partial fraction expansion to get the equivalent expression

$$g(x) = \sum_{i=1}^{L}\frac{A_i}{x-x_i}, \qquad \text{where } A_i = \frac{x_i^{L-2}}{\prod_{\substack{j=1\\ j\neq i}}^{L}(x_i-x_j)}. \tag{77}$$

Note that $A_i = B_i$. If we now reconsider (77) and write it again with a common denominator, we obtain a third form for $g(x)$

$$g(x) = \frac{\sum_{i=1}^{L} A_i \prod_{\substack{j=1\\ j\neq i}}^{L}(x-x_j)}{\prod_{i=1}^{L}(x-x_i)}. \tag{78}$$

The coefficient of x^{L-1} in the numerator in (78), which is equal to $\sum_{i=1}^{L} A_i$ must be equal to zero because of (76).

REFERENCES

[1] M. Schwartz, W. Bennett, and S. Stein, *Communication Systems and Techniques*. New York: IEEE Press, 1996.

[2] E. A. Lee and D. G. Messerschmitt, *Digital Communication*. Norwell, MA: Kluwer, 1994.

[3] J. Proakis, *Digital Communication*, 3rd ed. New York: McGraw-Hill, 1995.

[4] M. K. Varanasi and A. Russ, “Noncoherent decorrelative detection for nonlinear nonorthogonal modulation in Gaussian multiuser channels,” in *Proc. IEEE Int. Conf. Communications*, Montréal, QC, Canada, June 1997, pp. 919–923.

[5] E. Visotsky and U. Madhow, “Multiuser detection for CDMA systems with nonlinear modulation,” in *Proc. IEEE Int. Symp. Information Theory*, Ulm, Germany, July 1997, p. 355.

[6] M. L. McCloud and L. L. Scharf, “Generalized likelihood detection on multiple access channels,” in *Proc. 31st Annu. Asilomar Conf. Signals, Systems, and Computers*, Pacific Grove, CA, Nov. 1997, pp. 1033–1037.

[7] M. K. Varanasi and A. Russ, “Noncoherent decorrelative detection for nonorthogonal multipulse modulation over the multiuser Gaussian channel,” *IEEE Trans. Commun.*, vol. 46, pp. 1675–1684, Dec. 1998.

[8] M. K. Varanasi and D. Das, “Noncoherent decision feedback multiuser detection for nonlinear modulation,” *IEEE Trans. Commun.*, vol. 48, pp. 259–269, Feb. 2000.

[9] A. Russ and M. K. Varanasi, “Minimum error probability and suboptimum noncoherent multiuser detection for nonlinear nonorthogonal synchronous signaling over a Rayleigh fading channel,” in *Proc. IEEE Personal, Indoor, Mobile Radio Communications Conf.*, Helsinki, Finland, Sept. 1997, pp. 58–62.